Geomechanics and Engineering, *Vol. 33, No. 4 (2023) 341-352*
https://doi.org/10.12989/gae.2023.33.4.341

Experimental study on the horizontal bearing characteristics of long-short-pile composite foundation

Chen-yu Lv[a], Yuan-cheng Guo*, Yong-hui Li[b], An-di Hu-yan[c] and Wen-min Yao[d]

School of Civil Engineering, Zhengzhou University,
100 Science Avenue, Zhengzhou, Henan province, People's Republic of China

(*Received June 7, 2022, Revised February 27, 2023, Accepted March 16, 2023*)

Abstract. Long-short pile composite foundations bear both vertical and horizontal loads in many engineering applications. This study used indoor model tests to determine the horizontal bearing mechanism of a composite foundation with long and short piles under horizontal loads. A custom experimental device was developed to prevent excessive eccentricity of the vertical loading device caused by the horizontal displacement. ABAQUS software was used to analyze the influence of the load size and cushion thickness on the horizontal bearing mechanism. The results reveal that a large vertical load leads to soil densification and increases the horizontal bearing capacity of the composite foundation. The magnitude of the horizontal displacement of the pile and the horizontal load borne by the pile are related to the piles' positions. Due to different pile lengths, the long piles exhibit long pile effects and experience bending deformation, whereas the short piles rotate around a point (0.2 *L* from the pile bottom) as the horizontal load increases. Selecting a larger cushion thickness significantly improves the horizontal load sharing capacity of the soil and reduces the horizontal displacement of the pile top.

Keywords: horizontal bearing characteristics; horizontal load; long-short-pile composite foundation; model test; vertical load

1. Introduction

Industrialization has promoted geotechnical innovation, but complex engineering and geological problems require extensive attention. A composite foundation consists of piles with different lengths. Its mechanical properties are a combination of the properties of shallow and deep foundations. Long-short-pile composite foundations have higher bearing capacity and less soil settlement than pile foundations and are widely used in high-rise buildings (Liu *et al*. 2019). Academic research on composite foundations has mostly focused on vertical loads; however, large lateral loads may occur in buildings due to earthquakes, strong winds, or vehicle impact (Poorjafar *et al*. 2021, Ebadi-Jamkhaneh *et al*. 2021). The combination of different pile types and different horizontal load positions results in higher complexity of analyzing the horizontal bearing capacity of long-short-pile composite foundations than of traditional pile foundations. A complex pile-soil-cushion interaction occurs, and the stress and deformation characteristics of long and short piles are affected by the pile length, pile spacing, pile number, and cushion thickness, increasing the analysis complexity.

*Corresponding author, Professor
E-mail: guoyuancheng@163.com
[a]Ph.D. Student
[b]Associate Professor
[c]M.D. Student
[d]Ph.D.

Early research mainly focused on the vertical load-bearing mechanism of composite foundations, and provided meaningful results. These studies primarily focused on the bearing capacity and deformation settlement using theoretical analysis (Cheng *et al*. 2017, Xu *et al*. 2009), field or model tests (Wang *et al*. 2022, Miao *et al*. 2018, Wang *et al*. 2018), and numerical simulations (Moayed *et al*. 2013, Hazzar *et al*. 2017). The cushion thickness and pile material substantially affected the foundation settlement and vertical load sharing (Wang *et al*. 2018). Moreover, long piles had a more significant impact on the settlement and stiffness of composite foundations than short piles (Guo *et al*. 2021). However, due to the complex pile-soil-cushion interaction in long-short pile composite foundation, the horizontal bearing capacity has not been sufficiently investigated.

Theoretical research on foundations under horizontal loads has primarily focused on pile foundations. The current code adopts simplified calculation methods to calculate vertical and horizontal loads, and uses the small deformation superposition principle to calculate pile displacement and internal force (Oh *et al*. 2018). Scholars have proposed theoretical methods to determine the load-deformation characteristics of piles under a horizontal load. The most common methods are the subgrade reaction method (Rahgooy *et al*. 2022, Jeong *et al*. 2017), elastic continuum method (Gupta *et al*. 2017), and *p-y* method (Choo *et al*. 2016, Lovera *et al*. 2021, Mayoral *et al*. 2016), but existing analysis methods are limited. The most direct approach to studying horizontal bearing behavior is to carry out load tests. However, due to the complexity and uncertainty of field tests, most studies have used indoor

ISSN: 2005-307X (Print), 2092-6219 (Online)

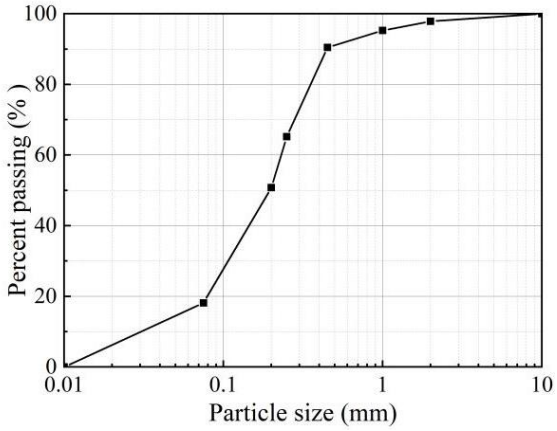

Fig. 1 Grain size distribution

model tests to analyze the internal force of the pile (Zhang *et al*. 2021, Gotman *et al*. 2018). The vertical load and the loading mode affect the horizontal bearing capacity of the pile. In addition, changing the pile top constraint type or developing new pile types can improve the horizontal bearing capacity (Vu *et al*. 2021, Ren *et al*. 2021).

This study investigates the horizontal bearing characteristics of a long-short-pile composite foundation. Four groups of long and short pile composite foundation tests are carried out to fill the research gap of a long-short-pile composite foundation under horizontal load. A sliding roller plate is designed to eliminate the influence of additional horizontal friction and prevent excessive eccentricity of the vertical loading device. The lateral displacement and bending moment of the pile are measured by displacement sensors and strain gauges. In addition, ABAQUS finite element software is used for a simulation, and the effect of different influencing factors on the horizontal bearing characteristics are analyzed.

2. Horizontal loading tests

2.1 Soil

Previous studies (Garnier *et al.* 2007, Floravante *et al*. 2002) have shown that the influence of the soil particle size can be ignored. Therefore, the soil used in the model test was the same as the prototype soil. The soil was filled in layers using the free-fall method, and the height of each layer was 150 mm. The sand in each layer was compacted with a plate vibrator, and the next soil layer was added. After the filling was completed, soil samples were obtained to test the basic soil properties. The model box was left for 7 days to allow the soil to settle. The soil moisture content was 0.64%, the cohesion was 6 kPa, and the internal friction angle was 30º. Fig. 1 shows the soil grain size distribution. The particle content of sand with a particle size greater than 0.075 mm accounted for 82.5% of the total weight; thus, the soil was classified as silty sand. A cushion layer with a thickness of 50 mm was added to the pile top. The roller plate and the loading plate were placed on top of the cushion; thus the raft was not contact with the pile heads.

Table 1 Model test parameters of the pile

Parameter	Symbol	Parameter	Scaling factor
Diameter	D (mm)	100	1 : 3
Length	L (mm)	1000/2100	1 : 3
Elastic modulus	E (GPa)	72	1 : 1
Density	ρ/(kg/m3)	2500	1 : 1

2.2 Model pile

The prototype of the model pile (the elastic modulus was 28 GPa, pile diameter was 300 mm, pile spacing was 4 D (D was the pile diameter) , and the length-diameter ratio was 21) was a C25 rigid concrete pile. Since the similarity ratio does not affect the stress level, an elastic modulus similarity ratio of 1 was used, and the scaling of the model pile length was 1:3. A hollow aluminum alloy tube was selected as the pile, its outer diameter was 100 mm, and the modulus was 72 GPa. The tube thickness and long pile length were 3 mm and 2100 mm, respectively. Since roughness of the pile affects the side friction, a knurling treatment was applied to the piles to reduce the roughness (Fig. 2).

A BX-120-5AA strain gauge was used to obtain the strain of the piles. It was attached to the middle of the pile with a vertical spacing of 200 mm, and the spacing on both sides was 100 mm (Fig. 3). Two strain gauges were placed in each section with an orientation in the horizontal loading direction to measure the stress changes on the front and rear sides of the pile body. There are 22 strain gauges on the long pile, and 12 strain gauges were attached to the short pile.

2.3 Model test system

The model test system consisted of four parts: a model box, loading system, reaction device system, and data measurement system. The large test model box (Fig. 4) was 2000 mm in length, 2000 mm in width and 4000 mm in height. Sixteen removable rectangular steel plates (100 mm × 160 mm × 10 mm) were attached with bolts to the side of the model box. The horizontal reaction frame was composed of H steel and square steel tubes welded together. It was tightly attached to the model box with high-strength bolts to enable disassembly and not affect the loading and unloading of the soil. A horizontal jack was attached to the H steel through the triangular frame so that the height could be changed. The pile spacing was 4 D. The configuration of the piles is shown in Fig. 5. The horizontal spacing between the surrounding box and the pile side was 7.5 D, and the distance between the pile bottom and the box was 7 D; thus, the boundary effects could be ignored (Liu *et al*. 2016, Hong *et al*. 2017).

When the vertical and horizontal loads were applied, the bearing plate caused horizontal displacement due to the horizontal force. The plate top was in close contact with the vertical jack, and the uneven settlement of the plate caused an inclination of the jack and eccentricity. A custom

Fig. 2 Rigid model pile

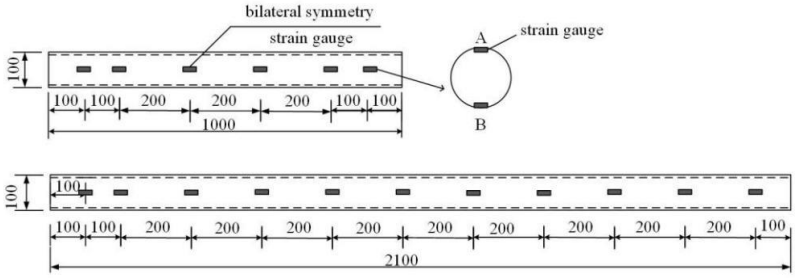

Fig. 3 Arrangement of the strain gauges of the piles (unit: mm)

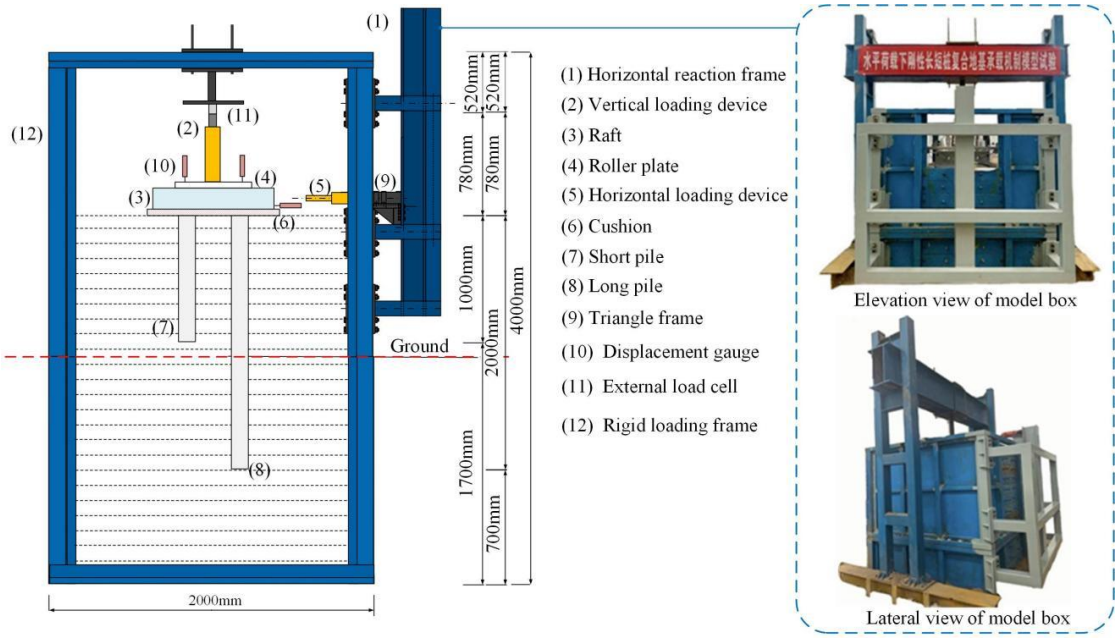

Fig. 4 Model test system

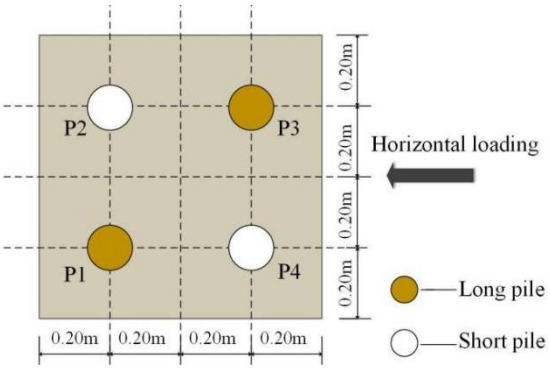

Fig. 5 Configuration of the four piles

designed sliding roller plate was placed on the top of the raft. It consisted of bearings and connecting plates, with a length of 600 mm in length, a width of 330 mm, and thickness of 60 mm. When the raft was horizontally displaced, the bearing of the roller plate moved horizontally, but the upper connecting plate did not. This design ensured that the vertical jack always remained vertical. Rigid composite foundations are typically not reinforced in practical engineering; the horizontal displacement cannot be ignored. The displacement gauge and the pile top were connected with iron wires to measure the horizontal displacement of the pile top, and the settlement on both sides of the loading plate was measured with four displacement gauges. The data from pressure sensors, strain gauges, and displacement meters were automatically corrected using a CM-2B static data acquisition instrument. Fig. 6 shows the measurement device.

2.4 Loading scheme

Four groups of load tests were conducted on the rigid long-short-pile composite foundation under horizontal

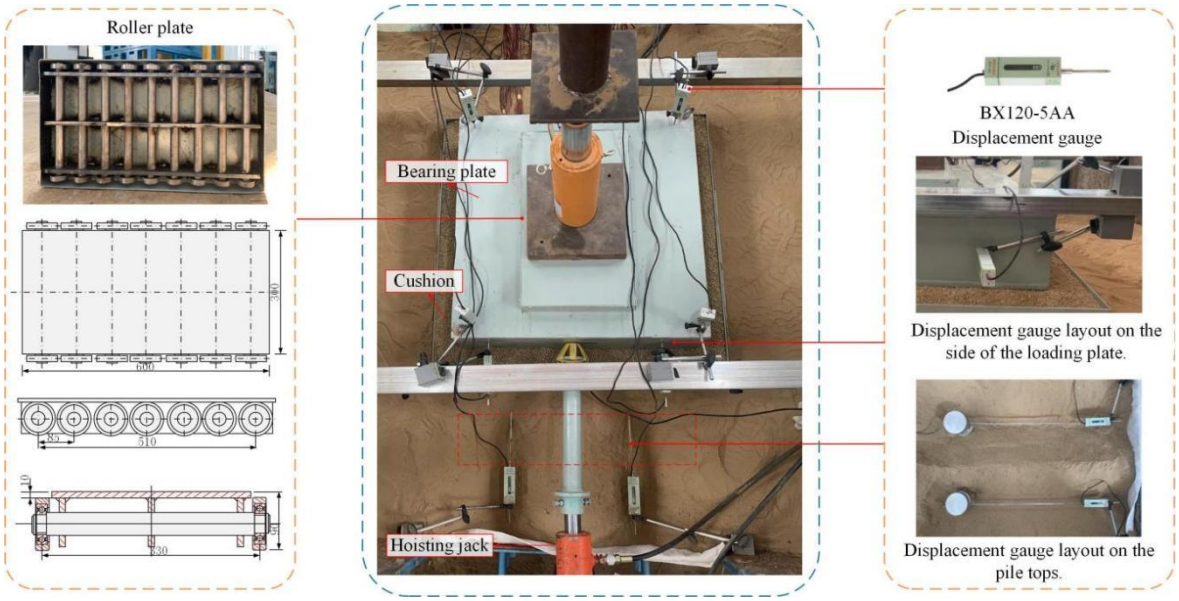

Fig. 6 Test device

Table 2 Loading scheme of the model test

Test number	Vertical load (kPa)	Horizontal load (kPa)
1	0-60	0
	60	0-H_{max1}
2	0-70	0
	70	0-H_{max2}
3	0-80	0
	80	0-H_{max3}
4	0-90	0
	90	0-H_{max4}

loads. The loading scheme is listed in Table 2. Vertical loads of 60 kPa, 70 kPa, 80 kPa, and 90 kPa were selected according to the characteristic value of the bearing capacity. The static load test was carried out in multiple stages. First, we applied the vertical load stepwise to the desired value. When the composite foundation was stable, the vertical load was kept constant, and a horizontal load of 2 kN was applied in each stage until the horizontal displacement of the loading plate increased sharply or the horizontal displacement of the raft was twice that of the upper layer at a certain level. At this time, it was assumed that the limit horizontal load had been reached, and the load was terminated. The pile near the horizontal loading side was defined as the back row pile (P3, P4), and the pile on the other side was the front row pile (P1, P2).

3. Results

3.1 Displacement of the composite foundation

Fig. 7 shows the overall settlement of the composite foundation when the vertical load is 90kPa. At vertical loads of 60 kPa, 70 kPa, 80 kPa, and 90 kPa, the corresponding horizontal load limits were 14 kN, 16 kN, 18

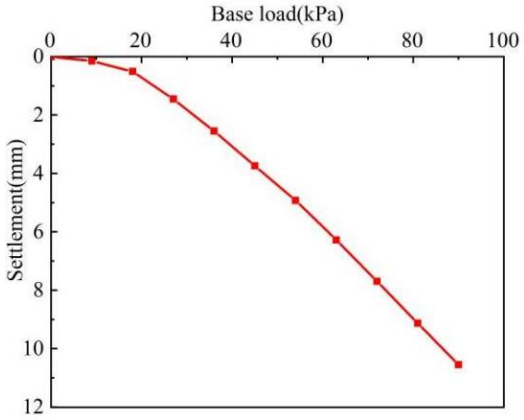

Fig. 7 Load settlement curves of the long-short-pile composite foundations

kN, and 22 kN, respectively. The horizontal bearing capacity increases with an increase in the vertical load. Increasing the vertical load can improve the effective vertical compressive stress of the soil between the piles, thereby improving the shear strength and the ultimate bearing capacity of the piles.

Fig. 8 shows the horizontal load and displacement curves of the raft and the pile top under different loads. The horizontal displacement of the raft is always larger than that of the pile top. As the horizontal load increases, the horizontal displacement increases. The pile, soil, and cushion share the load. The horizontal load is first transmitted to the cushion by friction and then to the piles and the soil between the piles. In addition, under the same horizontal load, changing the magnitude of the vertical load has a negligible effect on the horizontal displacement of the pile top, confirming the result of Wu *et al*. (1996), who found that the Q-U_p curve was consistent.

The horizontal load causes pile-soil separation in the composite foundation, thereby reducing the soil pressure

Table 3 Settlement at the top of the raft

Horizontal load/kN	0	4	8	12	16	20	22
Settlement on the left/mm	10.545	10.675	10.865	11.108	11.528	11.983	12.325
Settlement on the right/mm	10.545	10.625	10.785	10.932	11.018	11.188	11.298

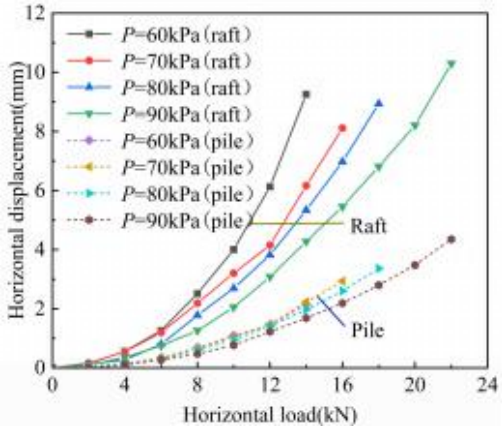

Fig. 8 The horizontal displacement at horizontal loads

and the pile side friction, leading to the additional settlement of the pile. The settlement on both sides of the raft (away from and near the horizontal loading side) is listed in Table 3. When V=90 kPa and H=0, the settlement on both sides of the raft is the same (10.545 mm). As the horizontal load increases, both sides continue to settle. When H=22 kN, the raft settlement away from the horizontal loading side is 12.325 mm, and that near the loading side is 11.298 mm. Therefore, as the horizontal load increases, the settlement difference on both sides of the raft gradually increases. In practical engineering, the influence of the foundation settlement difference must be considered when the superstructure is subjected to a large horizontal load to prevent the inclination of the structure.

3.2 Bending moment of the pile

The pile is compressed and bent under vertical and lateral loads, and the cross-section of the pile produces tensile and compressive strains. The bending moment is calculated from the strain of the pile. The bending moments of the piles under 90 kPa vertical load are shown in Fig. 9.

The bending moment curve of the pile is parabolic. The bending moment increases and then decreases in the depth direction. When the soil depth is less than 0.4 L (L is the length of the pile), the bending moment is mainly affected by the p-Δ effect. The pile experiences large horizontal displacement under a horizontal load. Due to the large vertical force on the upper part, additional horizontal soil resistance is generated near the pile, which is balanced with the bending moment generated by the lateral displacement of the pile. Therefore, as the depth increases, the bending moment of the pile decreases. The maximum bending moment of the long pile occurs at 0.4-0.6 m below the pile top, and the bending moment at the upper part is greater than that at the bottom. The maximum value of the short pile is about 0.4 m. Moreover, the bending moment is substantially lower than that of the long pile.

Fig. 9 shows a downward trend in the position of the maximum bending moment. When the horizontal load increases, the deep soil is fully mobilized, thereby improving the resistance to the horizontal load. The horizontal force is further transmitted to the deep soil, enhancing the horizontal bearing capacity of the composite foundation. When the horizontal load is applied for the first time, the bending moment of the back row pile is slightly larger than that of the front row pile. As the load continues to increase, uneven settlement of the raft occurs, and the growth rate of the bending moment of the front row piles increases. Finally, the bending moment of the front row piles is greater than that of the back row piles. In long-short-pile composite foundations, the curves of the piles with the same length are similar at different positions. The long pile shows a ‘long pile effect’, and the bending moment curve has many inflection points along the pile. In contrast, the short pile bending moment curve has a parabolic shape, and the values increase and then decrease in the depth direction. Under a larger horizontal load, the ranking of the piles’ bending moments is P1 > P3 > P2> P4.

Fig. 10 shows the shear force of the piles at different positions under 90 kPa vertical load. The shear force has a linear relationship with the upper depth, and the maximum value occurs near the pile top. Therefore, the shear failure of the pile is most likely to occur near the top. The shear force gradually decreases with an increase in the depth, and is 0 at about 0.4 m. When the depth exceeds 0.4 m, a reverse shear force is generated. Due to the soil resistance around the pile, the shear force near the bottom of the long pile is approximately 0. Furthermore, the trend of the shear force with the horizontal load is the same as for the pile’s bending moment. Under the maximum horizontal load, the maximum shear force of the front row long piles is about 1.47 times that of the back row; that of the short piles in the front row is 1.48 times that of the short piles in the back row.

4. Discussion

Due to limitations of the measurement method in the test, many measurement could not be obtained to analyze the horizontal bearing mechanism. Therefore, a numerical simulation model consistent with the model test parameters was established in the ABAQUS finite element software. The model was composed of the structural (pile and raft) and geotechnical parts (soil and cushion), and the elastic and ideal elastic -plastic Mohr-Coulomb constitutive models were used, respectively. It was assumed that the

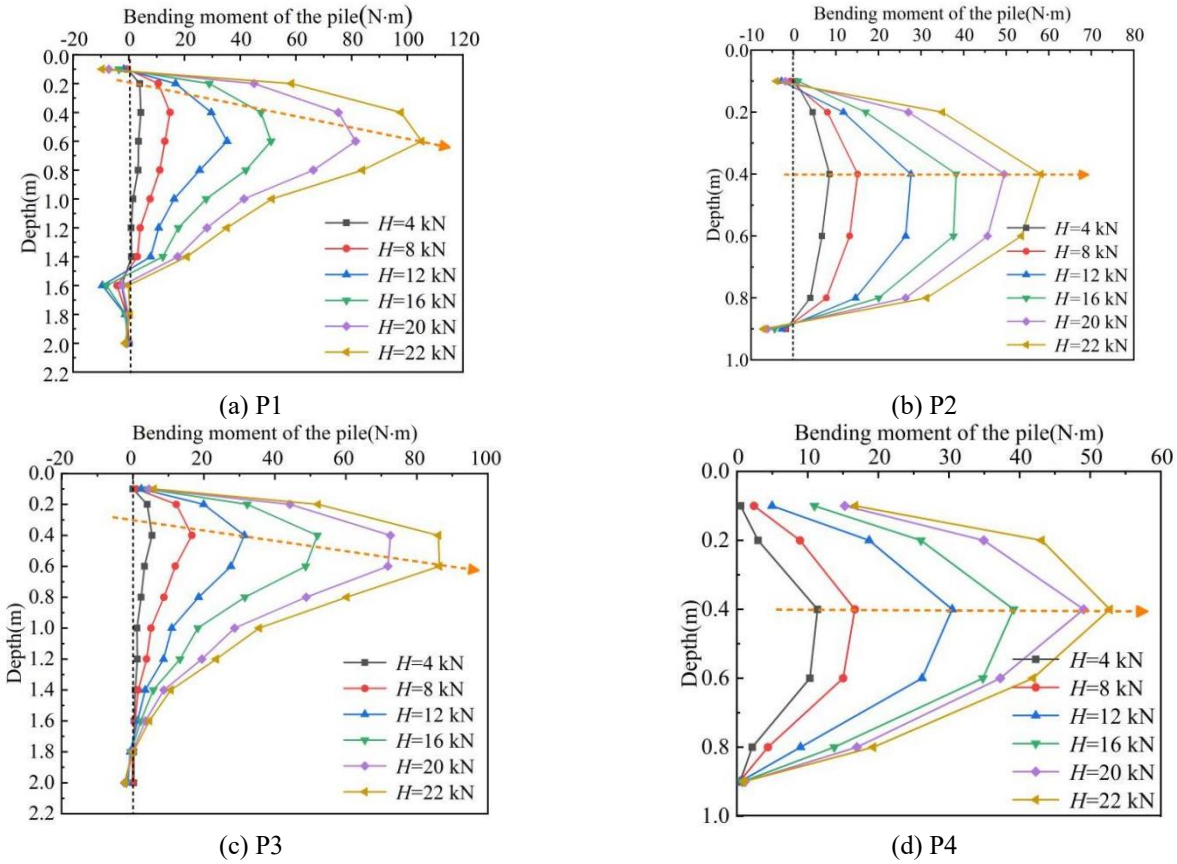

(a) P1 (b) P2

(c) P3 (d) P4

Fig. 9 The bending moments of the four piles under different horizontal loads (V=90 kPa)

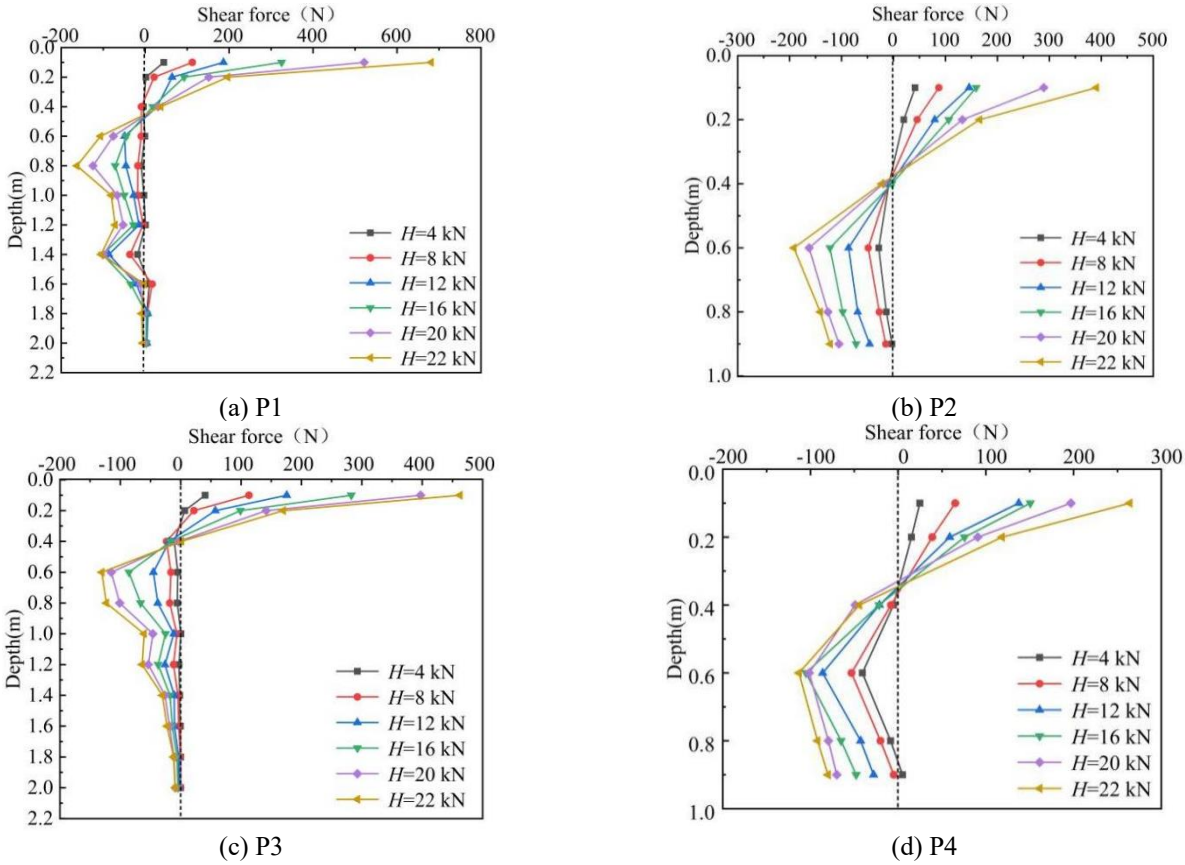

(a) P1 (b) P2

(c) P3 (d) P4

Fig. 10 The curves of the shear force of the piles under different horizontal loads (V=90 kPa)

Table 4 Model parameters employed in the finite element analysis

Parameter	ρ/(kg/m3)	E/(MPa)	v	c/(kPa)	φ/(°)
Soil	1600	20	0.3	6	30
Cushion	1400	30	0.3	4	33.9
Pile	2500	8100	0.2	-	-
Raft	7800	210000	0.2	-	-

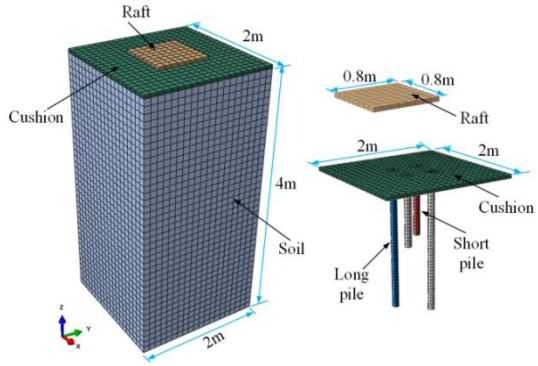

Fig. 11 3D numerical simulation model

cushion and soil were homogeneous media. Table 4 lists the material parameters obtained from the tests. The horizontal and vertical displacements of the soil bottom were constrained, and the surrounding area was subjected to horizontal constraints perpendicular to the side. There was no constraint on the upper surface of the soil. When the horizontal load was applied, the displacement in the X-direction of the cap was not constrained. Fig. 11 depicts the mesh; the mesh density was finer around the piles. A surface-to-surface contact was selected between the raft, cushion, pile, and soil, and the cushion was connected to the surrounding soil by a tie contact to simulate the real stress condition. Table 5 lists the friction coefficients of the interaction surfaces. The surface with a higher stiffness was the master surface, and that with a lower stiffness was the salve surface to ensure convergence. After the initial stress field was balanced, the pile, cushion, and raft were introduced sequentially by establishing the contacts at the interaction interface.

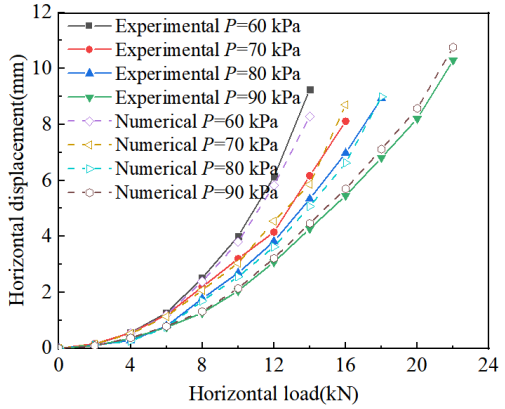

Fig. 12 Experimental and numerical horizontal settlement results of the raft

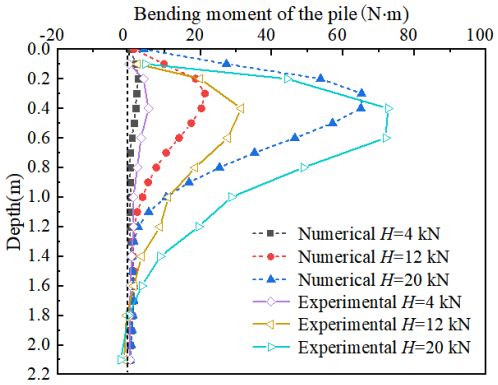

Fig. 13 Experimental and numerical horizontal bending moment of the pile (P1)

4.1 Numerical simulation verification

We compared the measured and simulated parameter val ues due to the complexity of the soil state and the uncertaint y of the soil parameters. Fig. 12 shows the horizontal displa cement of the raft obtained from the model test and numeric al simulation. Fig. 13 lists the calculation results of the bend ing moment of the front row pile under different horizontal l oads. The curves are in good agreement, and the small diffe rent are attributed to the fact that the indoor model test cann ot achieve the ideal conditions of the numerical simulation. The results verify the effectiveness of the numerical model.

4.2 Effect of the load on the horizontal bearing mechanism

The ratio of the horizontal load on each component to the total horizontal load is called the horizontal load-sharing ratio. Fig. 14(a) shows the horizontal load sharing ratio of the pile and soil at different horizontal loads (V=90 kPa). The results show that the soil bears most of the horizontal load, and the cushion also bears part of the horizontal load. Fig. 14(b) shows the horizontal load-sharing ratio of different rows of piles. The horizontal force increases from 4 kN to 22 kN, the horizontal load sharing ratio of the back row pile decreases from 58.3% to 45.7%, and that of the front row pile increases from 41.7% to 54.3%. The reason is the settlement difference on both sides of the raft. When the settlement difference is small, the back row piles bear more of the horizontal load initially. The proportion of the horizontal load on the front row piles increases with an increase in the horizontal load.

The stress deformation characteristics of the pile are related to the distance from the horizontal loading location. Fig. 15 lists the horizontal displacements of the four piles under different horizontal loads. There are considerable differences between the long and short piles, but the maximum values both occur at the pile top. The horizontal displacement of the long pile decreases with the depth, ranging from 0 to 0.8 m, and there is almost no horizontal displacement at the bottom (approximately 0), showing the long pile effect. The short pile rotates around a point at the bottom of the pile with an increase in the horizontal load,

Table 5 Contact parameters of the model

Contact surface	Contact type	Friction coefficient
Raft-cushion	surface-to-surface contact	0.365
Cushion-pile	surface-to-surface contact	0.82
Pile-soil	surface-to-surface contact	0.4
Cushion-soil	tie contact	-

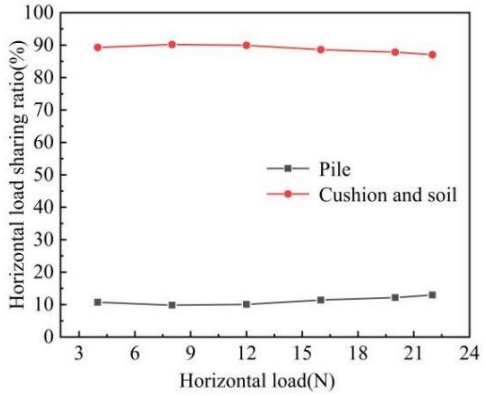

(a)

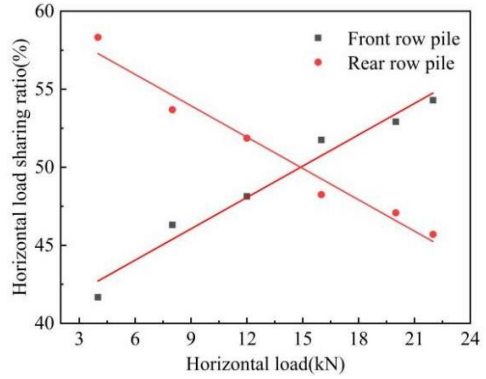

(b)

Fig. 14 The horizontal load sharing ratio of the (a) pile, cushion and soil and (b) the front row and rear row piles at different horizontal loads

and the horizontal displacement decreases with increasing depth. When it decreases to 0 and thenincreases in the opposite direction, the pile bottom has the reverse maximum value. Because the compressive stress of the short pile is small, the horizontal displacement directions of the upper and lower parts are the opposite.

In practical engineering, the piles in the composite foundation must bear the vertical load of the upper structure when it bears the horizontal loads. The compressive stress generated by the vertical load is balanced with the partial tensile stress of the pile. Four groups of different vertical loads were selected to determine stress deformation and load-sharing of the composite foundations under horizontal loads. Fig. 16 plots the horizontal load sharing ratio curves of the pile top under different loads. When the horizontal load is large, the effect of the vertical load is small. After the horizontal load exceeds 12 kN, the curve becomes linear.

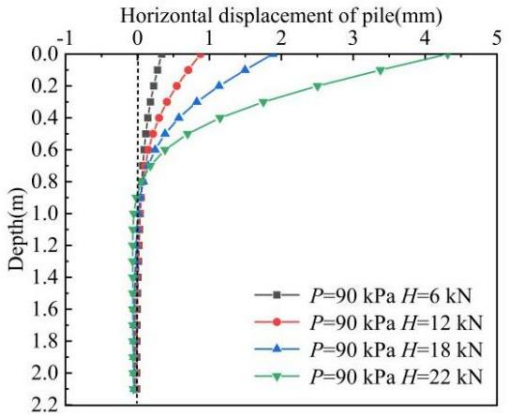

(a) P1

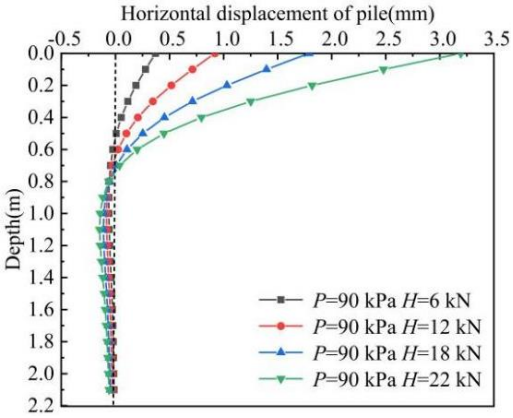

(b) P2

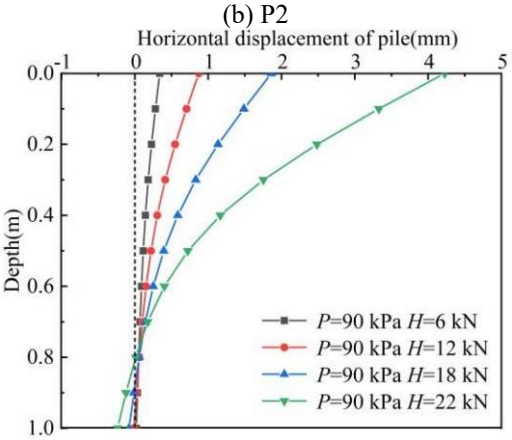

(c) P3

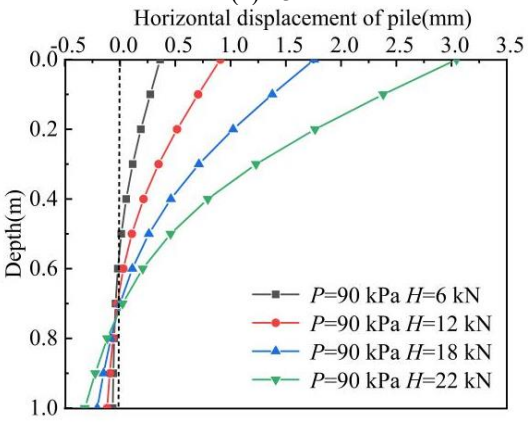

(d) P4

Fig. 15 The horizontal displacement of the piles under different loads

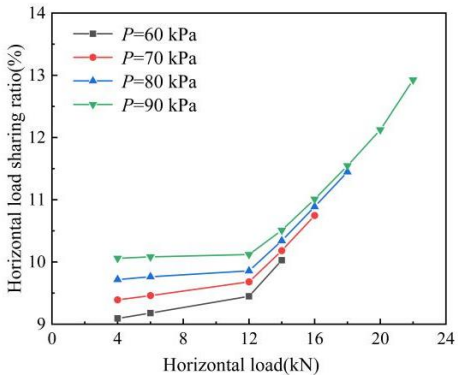

Fig. 16 The horizontal load sharing ratio of the pile top

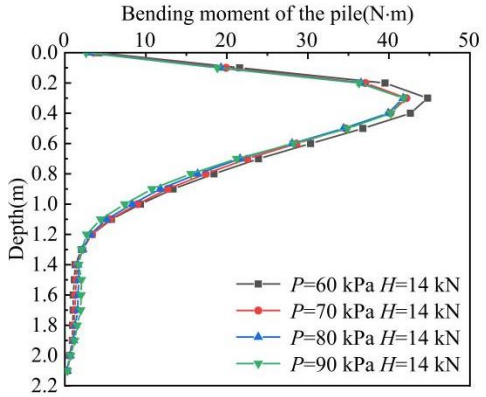

(a) P1

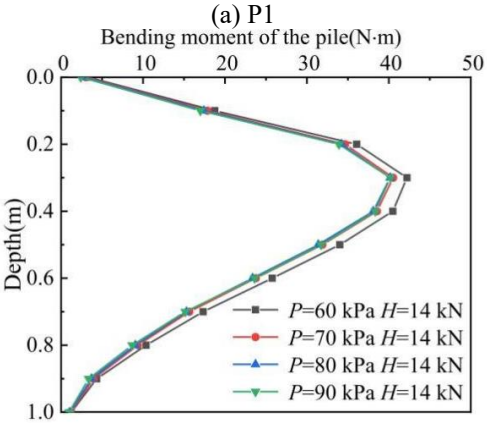

(b) P2

Fig. 17 The bending moment of the piles under different vertical loads (H=14 kN)

Fig. 17 shows the bending moment of the piles with different vertical loads under a horizontal load of 14 kN. The degree of soil compaction is closely related to the vertical load. As the load increases, the soil under and around the pile becomes denser, improving the ability of the soil to restrain the pile and resist horizontal deformation. At the depth of 1.2 m, the bending moment of the long pile decreases with an increase in the vertical load. However, when the depth exceeds 1.2 m, the influence of the load size on the bending moment negligible. The bending moment of the short pile decreases with an increase in the vertical load, but the rate of decrease is low. Thus, it is considered that the bending moment of the piles is only slightly affected by the vertical load.

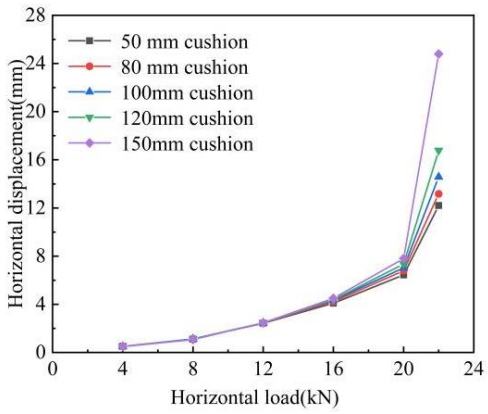

(a) Raft

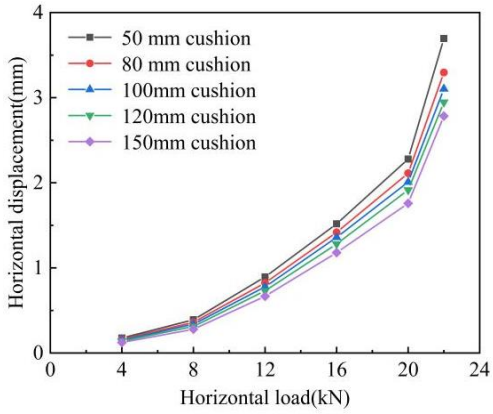

(b) Pile top

Fig. 18 The horizontal displacement of the pile for different cushion thicknesses

4.3 Effect of the cushion thickness on the horizontal bearing mechanism

The cushion is a key factor in distinguishing a composite foundation from a pile foundation. The change in the cushion thickness directly affects the horizontal bearing capacity. Therefore, the effect of different cushion thicknesses on the composite foundation at a vertical load of 90 kPa and a horizontal load of 22 kN was analyzed.

Fig. 18(a) shows the horizontal load-displacement curve of the raft. The increase in the cushion thickness leads to a higher horizontal displacement of the raft at the same horizontal load. The horizontal displacement at the top of the raft is almost the same under different cushion thicknesses at low horizontal loads. When the load exceeds 20 kN, the horizontal displacement increases sharply with an increase in the cushion thickness. The horizontal load-displacement curve of the pile top is shown in Fig. 18(b). As the cushion thickness increases, the horizontal displacement of the pile top gradually decreases. These results suggest that the fluidity of the soil in the cushion increases with cushion's thickness, and the cushion will be fully supplemented to the soil between the piles.

Fig. 19 shows the horizontal load-sharing ratio of the pile top. As the cushion thickness increases from 50 mm to 150 mm, the horizontal load-sharing ratio of the pile top is 6%-13%, and that of the soil is 87%-94%. The horizontal

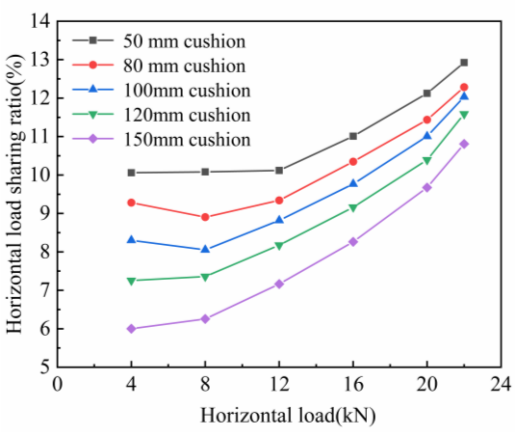

Fig. 19 The horizontal load sharing ratio of the pile top for different cushion thicknesses

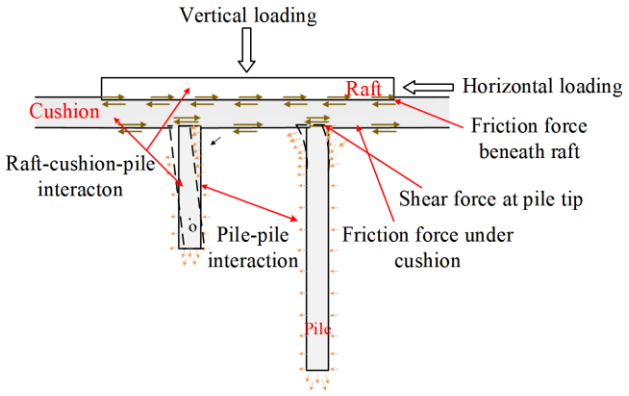

Fig. 20 Horizontal load distribution of the long-short-pile composite foundation under horizontal load

load on the pile top is inversely proportional to the cushion thickness. When the cushion thickness is 150 mm, the horizontal load shared by the pile is only 10.8% of the total horizontal load. Thus, increasing the thickness of the cushion ensures sufficient soil fluidity and shear deformation of the soil, thereby improving the safety of the piles.

4.4 Analysis of horizontal bearing mechanism

Fig. 20 shows the horizontal load distribution of the long-short-pile composite foundation under vertical and horizontal loads. Since the pile is a slender rod, it can withstand vertical and lateral forces. The ability of the pile to withstand horizontal loads is much smaller than its ability to withstand vertical loads. The cushion disconnects the bottom of the foundation from the pile. Therefore, the composite foundation does not rely as much on the pile to bear the upper load, but the soil bears more of the load through pile-soil interaction. The horizontal load acting on the foundation is first transferred to the cushion. Then, the load acting on the cushion is distributed to the piles and the soil between the piles.

The pile is deformed and displaced under the action of the horizontal force. The upper soil moves to the left, and a pile-soil separation area occurs at the backside of the pile. The soil rapidly flows into the gap, and the pile-side soil is displaced and compressed, resulting in active earth pressure. The soil is densified due to an increase in the vertical load, improving the bearing capacity of the composite foundation. The horizontal force acting on the pile is borne by the soil pressure on the pile side, and the displacement in the deep soil is small. The pile lengths are different in long-short-pile composite foundations. Therefore, the long and short piles produce different horizontal displacements under the same horizontal load, resulting in different stress mechanisms. The short pile rotates around a point (O) at the bottom of the pile axis, and the soil strength around the pile determines the horizontal bearing capacity. The length-diameter ratio of the long pile is larger than that of the short pile, and there are more than two zero displacement points in a long pile. Thus, the bending moment and displacement decrease rapidly in the downward direction of the pile. The lower end of the long pile is embedded in the soil, while the upper part of the pile experiences horizontal displacement and rotation.

The vertical load and the thickness of the cushion layer affect the horizontal bearing characteristics of the composite foundation. Increasing the vertical load and decreasing the cushion thickness can significantly improve the horizontal load-sharing ratio of the pile top. The cushion thickness has the most significant influence on the horizontal load-sharing, and the horizontal displacement of the pile top decreases as the thickness of the cushion increases. Changing the vertical load has a negligible effect on the bending moment of the pile.

5. Conclusions

An indoor model test was carried out to research the horizontal bearing performance of a composite foundation with rigid long and short piles. A roller plate was developed to prevent tilting of the vertical loading device under horizontal loading. The settlement, horizontal displacement, bending moment, and shear force of the pile were analyzed, and the horizontal load sharing between the pile and the soil was investigated with finite element software. The main conclusions are as follows:

• The existing vertical load improved the horizontal bearing capacity of the composite foundation. Under the same horizontal load, the larger the vertical load, the greater the horizontal bearing capacity of the composite foundation was, enabling the pile body to bear large horizontal loads. The bending moment of the pile decreased with an increase in the vertical load, and the maximum value occurred at 3 D below the pile top (D is the diameter of the pile).

• When the long-short pile composite foundation was subjected to vertical and horizontal loads, the maximum horizontal displacement of the pile occurred at the pile top, and the horizontal displacement curves of the long pile and the short pile were different. As the horizontal load increased, the short pile rotated around a point of the pile, whereas the long pile had multiple points with zero displacements, showing the characteristics of long elastic

piles.

• The difference in the horizontal load borne by the piles in the same row perpendicular to the horizontal load direction was small. In contrast, the back row piles bore most of the load in the initial stage of horizontal loading. As the horizontal load increased, a settlement difference occurred on both sides of the raft, and each row of piles entered the working state in turn in the horizontal loading direction. Ultimately, the front row piles bore more of the horizontal load.

• Increasing the cushion thickness utilized the fluidity and shear deformation ability of the soil so that the horizontal load was shared between the piles and the soil. The horizontal displacement of the pile top in the composite foundation decreased, and the horizontal load borne by the soil between the piles increased. As a result, the horizontal load borne by the pile decreased, reducing the potential for damage to the piles.

Conflicts of Interest

The authors declare that they have no known competing financial interests or personal relationships that could have appeared to influence the work reported in this paper.

Acknowledgments

This work was supported by the National Natural Science Foundation of China [grant number 51508522] and the Cultivation Fund of Zhengzhou University in 2021 [grant number JC21439018].

References

Cheng, X.S. and Jing, W. (2017), "Calculation models and stability of composite foundation treated with compaction piles", *Geomech. Eng.*, **13**(6), 929-946. https://doi.org/10.12989/gae.2017.13.6.929.

Choo, Y.W. and Kim, D. (2016), "Experimental development of the p-y relationship for large-diameter offshore monopiles in sands: centrifuge tests", *J. Geotech. Geoenviron. Eng.*, **142**(1), 04015058. https://doi.org/10.1061/(ASCE)GT.1943-5606.0001373.

Ebadi-Jamkhaneh, M., Homaioon-Ebrahimi, A., Kontoni, D.P.N. and Shokri-Amiri, M.(2021), "Numerical FEM assessment of soil-pile system in liquefiable soil under earthquake loading including soil-pile interaction", *Geomech. Eng.*, **27**(5), 465-479. https://doi.org/10.12989/gae.2021.27.5.465.

Floravante, V. (2002), "On the shaft friction modelling of non-displacement piles in sand", *Soil. Found.*, **42**(2), 23-33. https://doi.org/10.3208/sandf.42.2_23.

Garnier, J., Gaudin,C., Springman, S., Cullingan, S.M., Goodings, D., Konig, D., Kutter, B., Phillips, R., Randloph, M.F. and Thorel, L. (2017), "Catalogue of scaling laws and similitude questions in geotechni-cal centrifuge modeling", *Int. J. Phys. Modell. Geotech.*, **7**, 1-23. https://doi.org/10.1680/ijpmg.2007.070301.

Gotman, A.L. and Sokolov, L.Y. (2018), "Lateral Load Analysis of a Composite Pile", *Soil Mech. Found. Eng.*, **55**(2), 103-109. https://doi.org/10.1007/s11204-018-9510-8.

Guo, Y.C., Lv, C.Y. and Hou, S.Q. (2021), "Experimental study on the pile-soil synergistic mechanism of composite foundation with rigid long and short piles", *Mathe. Problem. Eng.*, 6657116. https://doi.org/10.16285/j.rsm.2017.0068.

Gupta, B.K. and Basu, D., (2017), "Analysis of laterally loaded short and long piles in multilayered heterogeneous elastic soil", *Soil. Found.*, **57**(1), 92-110. https://doi.org/10.1016/j.sandf.2017.01.007.

Hazzar, L., Hussien, M.N. and Karray, M.(2017), "Influence of vertical loads on lateral response of pile foundations in sands and clays", *J. Rock Mech. Geotech. Eng.*, **9**(2), 291-304. https://doi.org/10.1016/j.jrmge.2016.09.002.

Hong, Y., He, B. and Wang, L. (2017), "Cyclic lateral response and failure mechanisms of semi-rigid pile in soft clay: centrifuge tests and numerical modelling", *Can. Geotech. J.*, **54**(6), 806-824. https://doi.org/10.1139/cgj-2016-0356.

Jeong, S., Park, J., Hong, M. and Lee, J (2017), "Variability of subgrade reaction modulus on flexible mat foundation", *Geomech. Eng.*, **13**(5), 757-774. https://doi.org/10.12989/gae.2017.13.5.757.

Liu, P., Yang, G.H. and Fan, Z. (2016), "Experimental study on scale effect of rigid pile composite foundation", *Chinese J. Rock Mech. Eng.*, **35**(1), 187-200.

Liu, W., Yang, X.H. and Chen, WZ. (2019), "Analysis of deformation characteristics of long-short pile composite foundation in salt lake area, Iran", *Adv. Civil Eng.*, 5976540. https://doi.org/10.1155/2019/5976540.

Lovera, A., Ghabezloo, S. and Sulem, J. (2021), "Pile response to multi-directional lateral loading using *p-y* curves approach", *Géotechnique*, **71**(4), 288-298. https://doi.org/10.1680/jgeot.18.P.297.

Mayoral, J.M., Pestana, J.M. and Seed, R.B. (2016), "Multi-directional cyclic p-y curves for soft clay", *Ocean Eng.*, **115**, 1-18. https://doi.org/ 10.1016/j.oceaneng.2016.01.033.

Miao, L.C., Wang, F. and Lv, W.H. (2018), "A simplified calculation method for stress concentration ratio of composite foundation with rigid piles", *KSCE J. Civil Eng.*, **22**(9), 3263-3270. https://doi.org/10.1007/s12205-018-1558-5.

Moayed, R.Z., Izadi, E. and Mirsepahi, M. (2013), "3D finite elements analysis of vertically loaded composite piled raft", *J. Central South Univ.*, **20**(6), 1713-1723. https://doi.org/10.1007/s11771-013-1664-y.

Oh, D.W., Ahn, H.Y. and Lee, Y.J. (2018), "Behaviour of vertically and horizontally loaded pile and adjacent ground affected by tunnelling", *Geomech. Eng.*, **15**(3), 861-868. https://doi.org/10.12989/gae.2018.15.3.861.

Poorjafar, A., Esmaeili-Falak, M. and Katebi, H. (2021), "Pile-soil interaction determined by laterally loaded fixed head pile group", *Geomech. Eng.*, **26**(1), 13-25. https://doi.org/10.12989/gae.2021.26.1.013

Rahgooy, K., Bahmanpour, A., Derakhshandi, M. and Bagherzadeh-Khalkhali, A. (2022), "Distribution of elastoplastic modulus of subgrade reaction for analysis of raft foundations", *Geomech. Eng.*, **28**(1), 89-105. https://doi.org/10.12989/gae.2022.28.1.089.

Ren, L.W., Yang, Q.W. and Kong, G.Q. (2021), "Model tests on Y-shaped piles under compressive and lateral loading in saturated sand", *Geofluids*, 6978602. https://doi.org/10.1155/2021/6978602.

Vu, A.T., Matsumoto, T. and Pham, D.P. (2021), "Behaviours of batter-pile foundations subjected to combination of vertical load and cyclic horizontal loading", *Int. J. Geotech. Eng.*, **12**(5), 592-605. https://doi.org/10.1080/19386362.2021.1929696.

Wang, C.D.; Zhou, S.H.;Wang, B.L. and Guo, P.J. (2018), "Time effect of pile-soil-geogrid-cushion interaction of rigid pile composite foundations under high-speed railway embankments", *Geomech. Eng.*, **16**(6), 589-597.

https://doi.org/10.12989/gae.2018.16.6.589.
Wang, F.C., Li, J. and Tian, P.P. (2022), "Research on hoop capacity of composite foundation of discarded rubber tires", *Eur. J. Environ. Civil Eng.*, **26**(2), 779-801. https://doi.org/10.1080/19648189.2019.1679671.
Wang, Z.Z., Gong, W.M. and Xiao, G. (2018), "Field test on composite foundation with thick cushion and sand pile group", *Rock Soil Mech.*, **39**(10), 3755-3762. https://doi.org/10.16285/j.rsm.2017.0068.
Wu, C.L., Yan, M.L. and Yang, J. (1996), "Properties of CFG pile and its composite foundation under horizontal load", *Geotech. Investigation & Surveying*, **4**, 18-21.
Xin, X., Kwag, Y. and Chun, B. (2013), "Study on settlement calculation of the long-short pile composite foundation", *J. Korean Geoenviron. Soc.*, **14**(7), 13-18. https://UCI : G704-SER000001652.2013.14.7.003.
Zhang, X.L., Xue, J.Y. and Han, Y. (2021), "Model test study on horizontal bearing behavior of pile under existing vertical load", *Soil Dynam. Earthq. Eng.*, **147**, 106820. https://doi.org/10.1016/j.soildyn.2021.106820.

CC